5 LIPID METABOLISM IS DISRUPTED BY ALTERATIONS TO PNPLA3

5.1 Introduction

Lipidomics is defined as the large-scale study of lipid pathways and networks and is a powerful tool for understanding lipid metabolism. This technique uses mass spectrometry to quantify the thousands of lipid species within a cell at a given time. This data can then be used to deduce the effect of physiological perturbations on the interactions and dynamics of lipid species. By examining the relative abundance of lipid species between experimental groups, one can gain insight into the metabolic pathways that may be affected by changes in genotype or treatment type. Lipidomics, in conjunction with other "omics" studies such as transcriptomics, offers the opportunity to gain mechanistic insight into pathologies that affect lipid metabolism. Additionally, lipidomics studies have been undertaken in the clinical setting for several pathologies known to affect lipid metabolism in a pathogenic way, including obesity, NAFLD, diabetes, etc [124, 237-239]. Given this huge influx for data from the clinic, lipidomics analyses of experimental systems can be used to examine the authenticity of a given system by comparing the results to published results from human patients. Lipidomics offers the unique opportunity to contextualize an *in vitro* system or murine model in terms of the human physiology and disease, making it an important tool to confirm the veracity of results discovered in these systems.

Due to the acute clinical interest in the PNPLA3 I148M variant and the lack of clarity on its mechanism of action, several clinical lipidomic studies have been undertaken in an attempt to parse the pathogenic mechanisms involved in PNPLA3-induced NAFLD [124, 126, 165, 237, 240]. These studies have revealed that PNPLA3 I148M carriers have vastly different lipidomic profiles than non-carriers of the risk allele with either a healthy metabolic profile or NAFLD caused by obesity rather than the variant. There are two main lipidomic changes in carriers of the risk allele: (1) reduced hepatic retention of lipotoxic and insulin resistance-inducing intermediates and (2) inversion of the PUFA concentration profile in triglycerides and phospholipids [126, 165].

Patients with obesity-associated NAFLD have increased concentrations of SFAs and SFA-containing triglycerides, ceramides, and diglycerides in their livers [237]. These lipid species are implicated in insulin resistance as well as lipotoxicity. Thus, the increased concentrations of these toxic intermediates in the livers of NAFLD patients

offers insight into the mechanisms of disease progression. While the absence of these lipids in the livers of I148M carriers dissociates potential mechanism of PNPLA3-induced NAFLD from that of obesity-induced NAFLD.

I148M carriers have reduced accumulation of triglycerides containing SFAs in their hepatocytes. This is due in large part to a reduction in de novo lipogenesis in these patients as well as increased secretion of SFA-containing triglycerides in VLDL. I148M carriers tend to have lower circulating concentrations of VLDL but they are uniquely enriched for SFAs [126, 165, 241]. This reduced hepatic SFA concentration also results in reduced de novo synthesis of ceramides. Ceramides are critical cell membrane components that play an important role in signalling as well. These lipids have been implicated in insulin resistance, oxidative stress, inflammation, and lipotoxicity. Ceramides are the primary mediators of insulin resistance in the liver. They activate protein kinase C which in turn activates lipogenic and lipid uptake processes. Simultaneously, ceramides impair AKT-mediated regulation of hepatic glucose production. Ceramides also play a key role in lipotoxicity. The accumulation of C16 ceramide derivatives perturbs calcium homeostasis which induces ER stress, the unfolded protein response, and ultimately cell death. Additionally, ceramides have been shown to interact with TNFα to promote the production of ROS, hepatic inflammation, and apoptosis. Thus, the reduction of ceramide concentrations has the dual benefit of reducing liver injury and improving insulin response [64, 79, 80]. Further, I148M carriers also have reduced hepatic concentrations of another key inducer of insulin resistance: diglycerides [124, 137]. Diglycerides are implicated in insulin resistance by stimulating protein kinase C to inhibit both PI3K and AKT signalling pathways. The reduced concentration of hepatic ceramides and diglycerides corresponds to the lack of metabolic syndrome often observed in patients with the I148M variant [57, 124, 137, 237, 242].

This discovery also demonstrates that PNPLA3-induced NAFLD has a unique pathogenic mechanism that is completely dissociated from that of obesity-induced NAFLD. In patients with obesity induced NAFLD, insulin resistance and increased de novo lipogenesis lead to the accumulation of lipid intermediates that exacerbate insulin resistance and lead to lipotoxicity and inflammation. Meanwhile, patients with PNPLA3-

induced NAFLD have reduced de novo lipogenesis and are more likely to escape metabolic dysfunction caused by insulin resistance. Thus, disease progression in these patients must be mediated by an, as yet, undiscovered perturbation to lipid metabolism.

PNPLA3 has been hypothesized to play in important role in lipid droplet remodelling by removing PUFAs from triglycerides and transferring them to phospholipids [127]. The I148M variant is believed to result in a loss of this remodelling capacity. In support of this hypothesis, patients with the I148M variant have increased hepatic retention of PUFA-containing triglycerides with a concomitant reduction in PUFA-containing phospholipids [165]. This pattern of PUFA accumulation may have profound effects on the lipid metabolism of these cells. First, the accumulation of PUFA in hepatic triglycerides leads to the inhibition of SREBP1c which causes downregulation of de novo lipogenesis [243, 244]. The reduction in de novo lipogenesis prevents the accumulation of toxic intermediates such as SFAs, ceramides, and diglycerides. By preventing the accumulation of these intermediates, carriers of the I148M variant are less likely to develop insulin resistance. The lack of insulin resistance as well as the presence of PUFAs per se reduces the apoptotic and inflammatory effect of lipid overload in hepatocytes [245-247]. Therefore, the lipid profile of steatotic livers from I148M patients is functionally distinct from those of obese patients. Since the increased steatosis in these patients cannot be accounted for by increased de novo lipogenesis as in obese patients, this triglyceride accumulation must result from a different mechanism.

The reduction of PUFA concentration in the phospholipids that comprise the lipid droplet membranes may offer some insight into this phenomenon. Lipid droplets are extremely dynamic organelles that maintain a diverse number of specific lipid droplet proteins based upon the temporal needs of the cell. The lipid composition of the membranes surrounding these organelles plays an important role in recruiting the appropriate proteins to the surface of the lipid droplet in order to maintain the balance between triglyceride synthesis and hydrolysis at any given time [248]. By altering the phospholipid composition of these membranes, PNPLA3 may be influencing the protein composition on the surface of the lipid droplet thereby disrupting the homeostasis between triglyceride anabolism and catabolism or restricting the mobility of these lipid species which results in the

sequestration of triglycerides in lipid droplets [128, 143]. Additional studies are needed to understand the mechanistic role of altered patterns of PUFA accumulation in the pathogenesis of PNPLA3-induced NAFLD.

In this chapter, we sought to harness the power of lipidomics to better understand the mechanism of lipid accumulation and escape from lipid induced stress by PNPLA3 edited cells. In addition, we used published lipidomic profiles from patients who are homozygous carriers of the I148M variant to validate lipidomic data from our *in vitro* system. The PNPLA3^{UC}, PNPLA3^{I148M}, and PNPLA3^{KO} lines were differentiated into HLCs, placed into 3D culture, and treated with either control, oleic acid, or palmitic acid medium for one week. Following the one-week treatment, intracellular lipids were extracted and analysed using mass spectrometry We then compared the differences in lipidomic profiles between the PNPLA3 edited and untargeted control lines to gain mechanistic insight into the phenotypes of these lines. We examined the triglyceride profiles of each of the PNPLA3 lines to identify lipid species that may play a role in lipid accumulation as well as reduced lipotoxicity of SFAs. In addition, we compared the lipidomic profile of the PNPLA3^{I148M} cells to patient data from I148M carriers in order to verify the results in our system in the context of human disease. We also tested the hypothesis that blocking triglyceride synthesis would re-sensitize PNPLA3-edited cells from both the FSPS13B and A1ATDR/R backgrounds to palmitic acid-induced lipotoxicity.

5.2 PNPLA3 edited lines have altered lipidomic profiles

In the previous chapter, we showed that alterations to the *PNPLA3* genotype resulted in profound effects on the lipid metabolism of HLCs. In order to more deeply analyse the differences in lipid metabolism caused by alterations to PNPLA3, we undertook lipidomic analyses of these cells. HLCs from each of the genotypes were treated with control or fatty acid medium for one week in order to maximize the steatotic phenotype of the cells and amplify the differences in lipid composition between genotypes. All lipidomic analyses were performed on lines derived from the FSPS13B background. For maximum clarity, the PNPLA3^{I148M} and PNPLA3^{KO} cells were compared individually to the PNPLA3^{UC} cells. This was done because the PNPLA3^{I148M} and PNPLA3^{KO} cells were

analysed at different times, in different mass spectrometry batches. The batch correction was attempted but it drastically altered the data sets as only 30% of the lipid species analysed were present in both batches. Consequently, we determined that it would be best to analyse the two genotypes separately with respect to the PNPLA3^{UC} cells in the same batch. Therefore, it is not possible to make direct, quantitative comparisons between PNPLA3^{I148M} and PNPLA3^{KO} cells. The analysis of the mass spectrometry data was performed using the publicly available online analysis pipeline Metaboanalyst [249, 250]. Given the observed phenotypes of each line and the working definition of the I148M variant as a loss of function variant, we hypothesized that the lipidomic profiles of the PNPLA3^{KO} and PNPLA3^{I148M} cells would be similar.

The overall lipidomic differences between PNPLA3^{KO} and PNPLA3^{UC} cells and between PNPLA3^{I148M} and PNPLA3^{UC} cells can be found in Figures 5.1 and 5.2, respectively. The PCA plots and heatmaps comparing the PNPLA3 edited cells to the untargeted control cells demonstrate that although fatty acid treatment alters lipidomic profiles significantly, the main determinant in lipidomic differences is genotype. There is relatively clear distinction between fatty acid treatments in PNPLA3^{UC} cells; however, this distinction is less clear in PNPLA3^{KO} and PNPLA3^{I148M} lines. These results track with the previous data showing that PNPLA3 edited cells fail to properly distinguish between SFAs and MUFAs when partitioning fatty acids for metabolism and storage. When examining the top 25 differentially abundant lipid species for PNPLA3^{KO} and PNPLA3^{I148M} cells compared to PNPLA3^{UC} cells, it is clear that the largest lipidomic differences are driven by triglycerides which is in accordance with previous studies that have shown that the I148M variant causes increased accumulation of hepatic triglycerides [126, 134, 150, 165].

In order to more precisely examine the lipidomic differences between genotypes, we separated the analyses by treatment type. Figure 5.3 shows the results of these analyses for the PNPLA3^{KO} line while Figure 5.4 shows the results for the PNPLA3^{I148M} line. These results further illustrate the marked lipidomic differences between PNPLA3^{KO} and PNPLA3^{UC} cells. Regardless of treatment type, the PNPLA3^{KO} cells cluster completely separately from PNPLA3^{UC} cells in PCA analyses. There is significantly more overlap

between PNPLA3^{I148M} and PNPLA3^{UC} cells in the same analysis. This indicates that the PNPLA3^{I148M} cells may once again represent an intermediate phenotype between PNPLA3^{UC} and PNPLA3^{KO} cells. Further, the number of differentially abundant lipid species between PNPLA3^{KO} HLCs and PNPLA3^{I148M} HLCs compared to their respective PNPLA3^{UC} HLCs supports the conclusions drawn from the PCA plots. The number of differentially abundant lipid species in PNPLA3^{KO} cells treated with control, oleic acid, and palmitic acid were 70, 71, and 59 respectively. There was a total of 788 lipid species included in the analysis therefore, 8.9%, 9%, and 7.5% of all lipid species were differentially expressed in PNPLA3^{KO} cells treated with control, oleic acid, and palmitic acid, respectively. The number of differentially abundant lipid species in PNPLA3^{I148M} cells treated with control, oleic acid, and palmitic acid were 77, 58, and 38, respectively. There were 910 lipid species included in this analysis. Thus, 8.4%, 6.3%, and 4.2% of the lipid species were differentially expressed in PNPLA3^{I148M} cells treated with control, oleic acid, and palmitic acid, respectively. This analysis indicates that alterations to PNPLA3 profoundly affects the lipidomic profile of HLCs and that the complete loss of PNPLA3 has a larger effect than the I148M variant, in accordance with previous results.

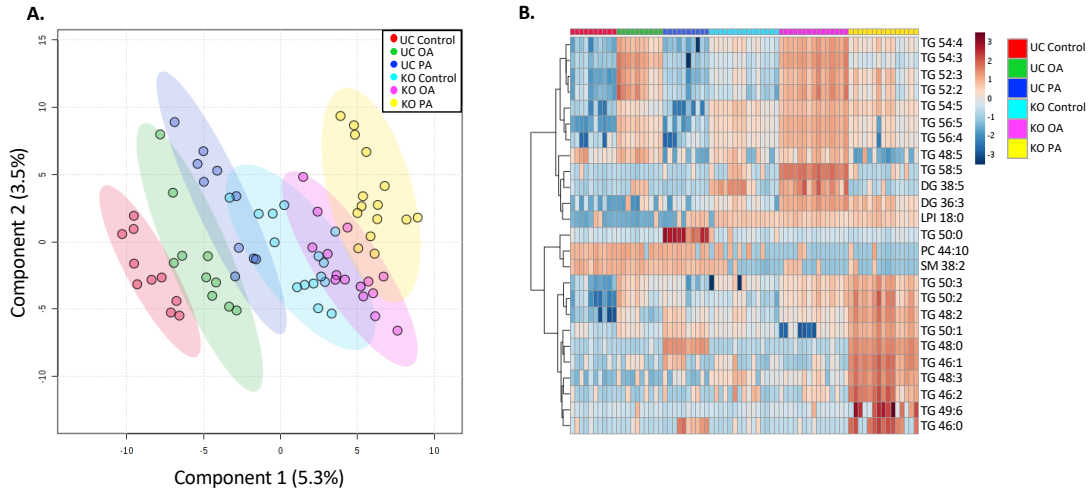

Figure 5.1 Lipidomic overview comparing PNPLA3^{KO} and PNPLA3^{UC} cells.

A. PLSDA plot of the 6 experimental groups (PNPLA3^{UC}: n = 2 clones (with 5 technical replicates) and 1 independent experiment; PNPLA3^{KO}: n = 3 clones (with 5 technical replicates) and 1 independent experiment). The two genotypes cluster separately with some differences attributable to the FFA treatment within each genotype. **B.** Heatmap of the top 25 differentially abundant lipid species in all 6 experimental groups. The lipid species most responsible for lipidomic differences between groups is triglycerides.

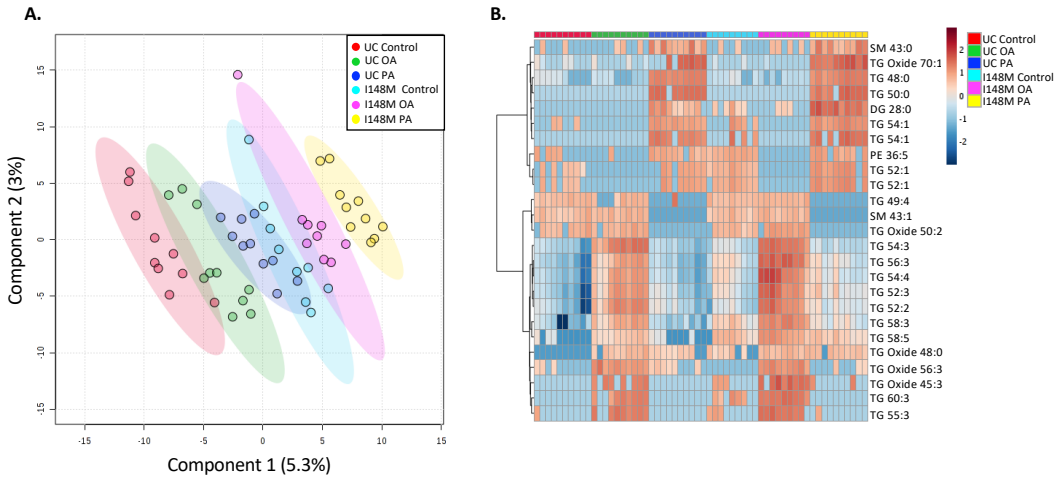

Figure 5.2 Lipidomic overview comparing PNPLA3^{I148M} and PNPLA3^{UC} cells.

A. PLSDA plot of the 6 experimental groups (PNPLA3^{UC}: n = 2 clones (with 5 technical replicates) and 1 independent experiment; PNPLA3^{I148M}: n = 2 clones (with 5 technical replicates) and 1 independent experiment). The two genotypes largely cluster separately with some differences attributable to the FFA treatment within each genotype. **B.** Heatmap of the top 25 differentially abundant lipid species in all 6 experimental groups. Triglycerides and their resultant oxides are the lipid species most responsible for differentiating the lipidomic profiles of the respective groups.

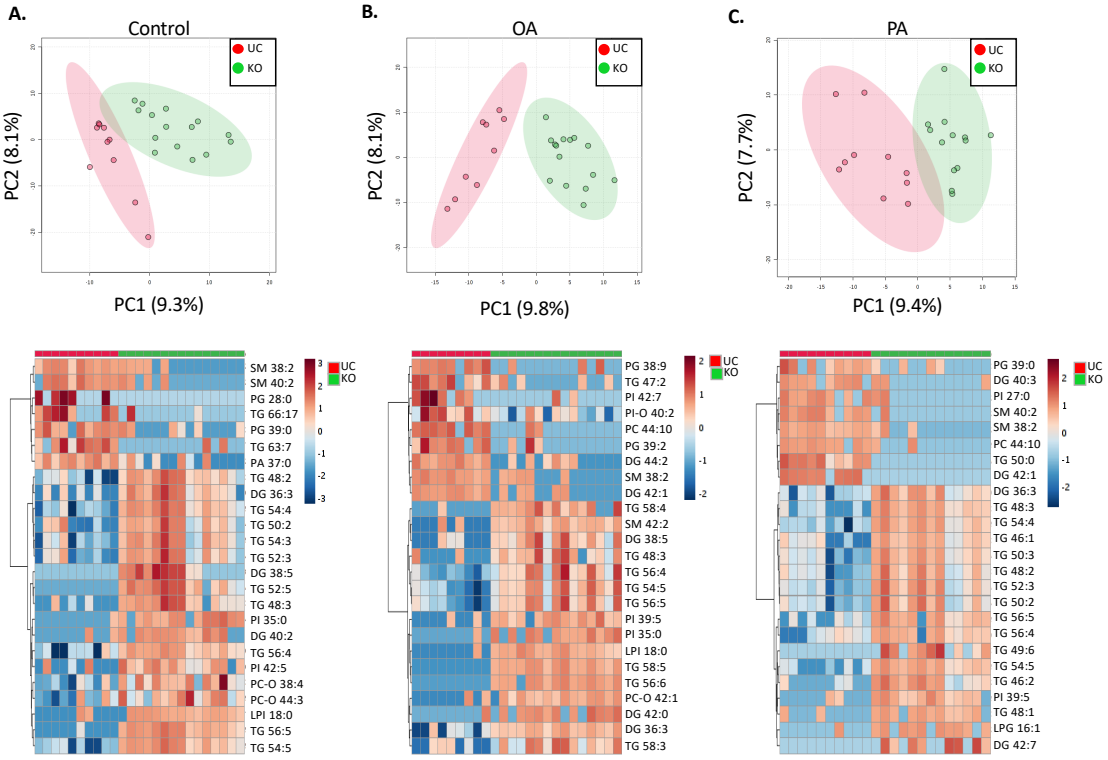

Figure 5.3 Lipidomic comparison of PNPLA3^{KO} and PNPLA3^{UC} cells separated by treatment.

PCA plots and heatmaps of the top 25 differentially abundant lipid species comparing the effect of media treatment on genotypic differences ($PNPLA3^{UC}$: n = 2 clones (with 5 technical replicates) and 1 independent experiment; $PNPLA3^{KO}$: n = 3 clones (with 5 technical replicates) and 1 independent experiment). Regardless of treatment, $PNPLA3^{UC}$ and $PNPLA3^{KO}$ cells clustered far apart from one another. Once again, triglycerides were a major determinant in driving lipidomic differences between the groups. **A.** $PNPLA3^{UC}$ and $PNPLA3^{KO}$ cells treated with control media. **B.** $PNPLA3^{UC}$ and $PNPLA3^{KO}$ cells treated with oleic acid. **C.** $PNPLA3^{UC}$ and $PNPLA3^{KO}$ cells treated with palmitic acid.

Upon closer examination of the lipid species comprising the top 25 differentially abundant lipid species in each treatment group for the two examined genotypes, several interesting trends appeared. In general, the PNPLA3-edited lines had a higher abundance of most examined lipid species. This trend was most clear when examining the triglyceride species. Interestingly, there were a few classes of lipids that were downregulated in the PNPLA3-edited cells. Of the few lipid species that were downregulated in PNPLA3-edited cells, diglycerides and sphingomyelins were the most common. Sphingomyelins are membrane components that are derived from phosphocholines and ceramides [251]. Therefore, a reduced accumulation of both diglycerides and sphingomyelins is consistent with the known lipidomic signatures of I148M patients.

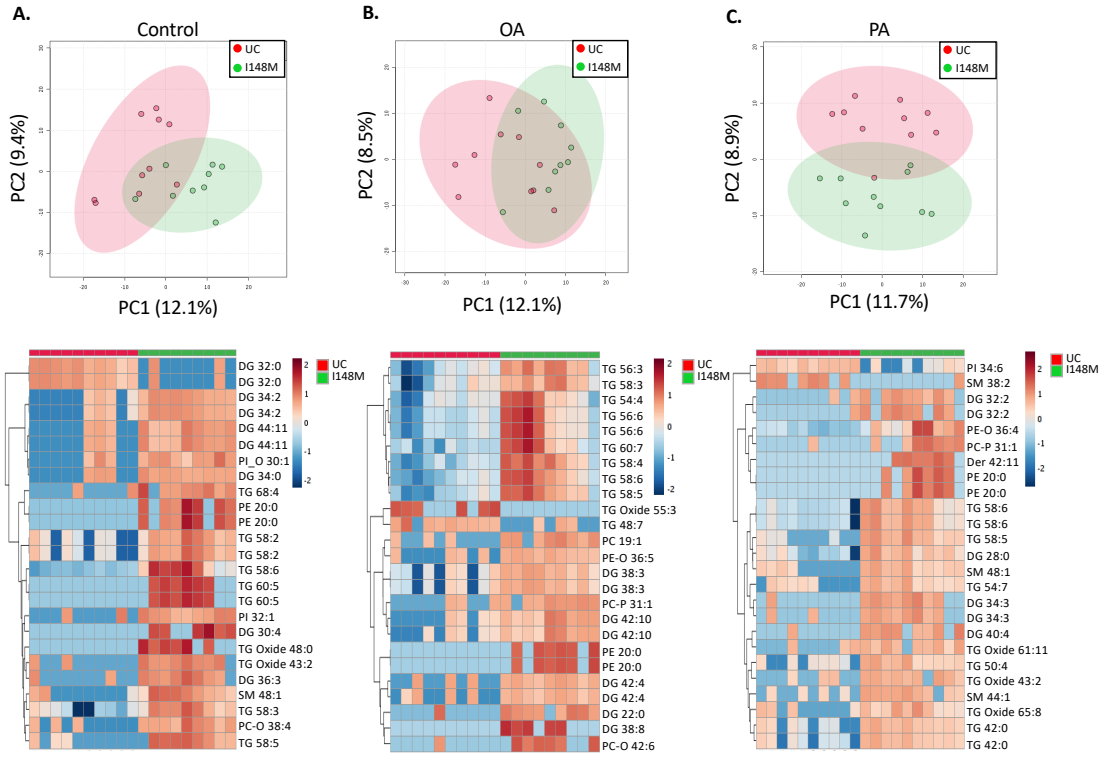

Figure 5.4 Lipidomic comparison of $PNPLA3^{I148M}$ and $PNPLA3^{UC}$ cells separated by treatment.

PCA plots and heatmaps of the top 25 differentially abundant lipid species comparing the effect of media treatment on genotypic differences ($PNPLA3^{UC}$: n = 2 clones (with 5 technical replicates) and 1 independent experiment; $PNPLA3^{I148M}$: n = 2 clones (with 5 technical replicates) and 1 independent experiment). There is some overlap between $PNPLA3^{UC}$ and $PNPLA3^{I148M}$ cells that varies depending on treatment type. Palmitic acid treatment appears to create the most lipidomic differences between the groups. Triglycerides as well as diglycerides were major determinants in driving lipidomic differences between the groups. **A.** $PNPLA3^{UC}$ and $PNPLA3^{I148M}$ cells treated with control medium. **B.** $PNPLA3^{UC}$ and $PNPLA3^{I148M}$ cells treated with oleic acid. **C.** $PNPLA3^{UC}$ and $PNPLA3^{I148M}$ cells treated with palmitic acid.

Given that the most differentially abundant lipid species in all treatment groups, regardless of genotype, were triglycerides, we decided to examine the triglyceride profile of the cells in more depth. We hypothesized that triglycerides are the key lipid mediators of PNPLA3 genotype on lipid metabolism, and the $PNPLA3^{KO}$ and $PNPLA3^{I148M}$ cells would preferentially accumulate triglycerides containing PUFAs. Additionally, given the results in Chapter 4, we hypothesized that the PNPLA3-edited cells would accumulate more triglycerides containing SFAs when treated with palmitic acid. The implications of these hypotheses will be discussed in more detail in the following sections. Heatmaps of the significantly differentially abundant triglyceride species between $PNPLA3^{KO}$ and $PNPLA3^{UC}$ cells in each treatment group can be found in Figure 5.6 while the corresponding heatmaps comparing $PNPLA3^{I148M}$ cells and $PNPLA3^{UC}$ cells can be found in Figure 5.7. An explanatory diagram to assist with the interpretation of these triglyceride heatmaps can be found in Figure 5.5.

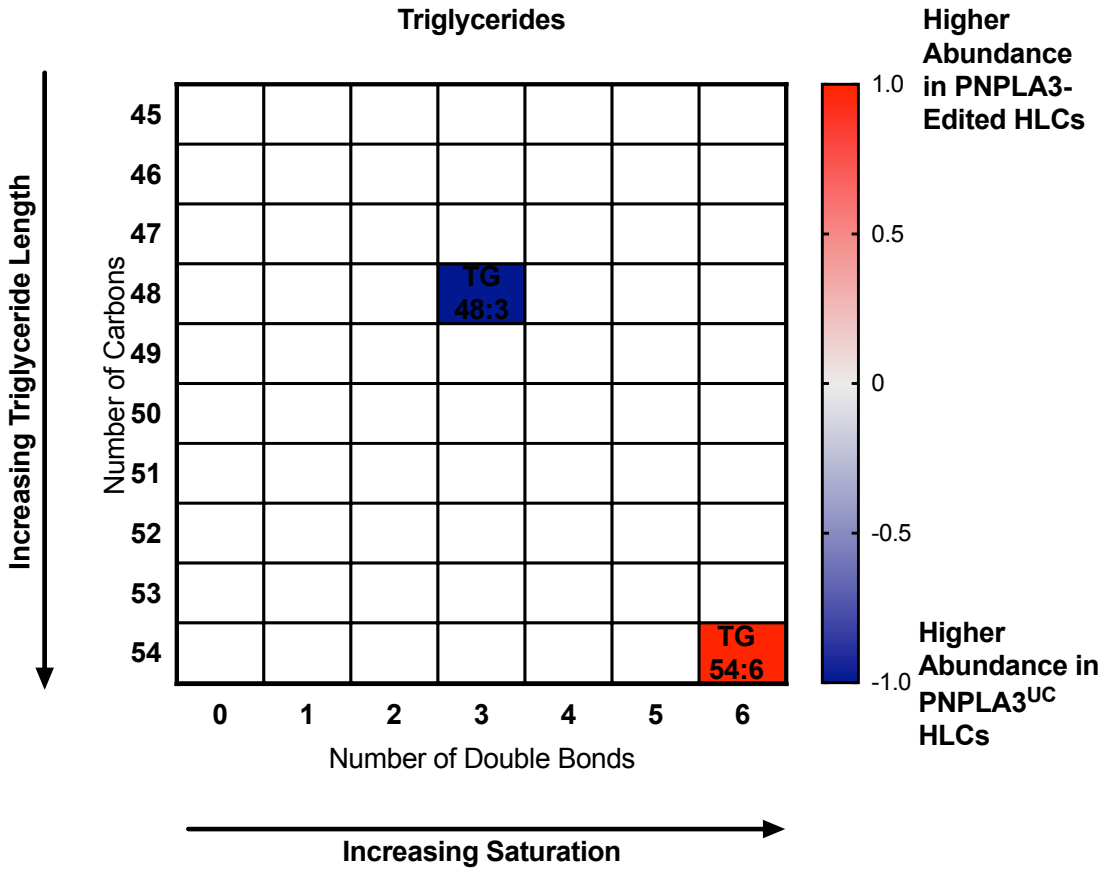

Figure 5.5 Explanatory diagram to assist with the interpretation of Figures 5.6 and 5.7.

This diagram represents a heatmap that shows differentially abundant triglyceride species between PNPLA3-edited and PNPLA3^{UC} HLCs. The Y-axis shows the number of carbons in the triglyceride so as one moves down the graph, the length of the triglyceride represented increases. The X-axis shows the number of double bonds in the triglyceride so as one moves across the graph, the saturation of the triglyceride represented increases. Any triglyceride species with 0-2 double bonds contains at least one saturated fatty acid while any species with 4 or more double bonds contains at least one polyunsatured fatty acid. Each box in the graph represents a single triglyceride. If the box is coloured white, the triglyceride is not differentially abundant between the two groups. If the box is coloured red, the triglyceride is more highly abundant in the PNPLA3-edited HLCs. If the box is coloured blue, the triglyceride is more highly abundant in the PNPLA3^{UC} HLCs. Therefore, in this example, TG 48:3 is more abundant in the PNPLA3^{UC} HLCs while TG 54:6 is more abundant in the PNPLA3-edited cells.

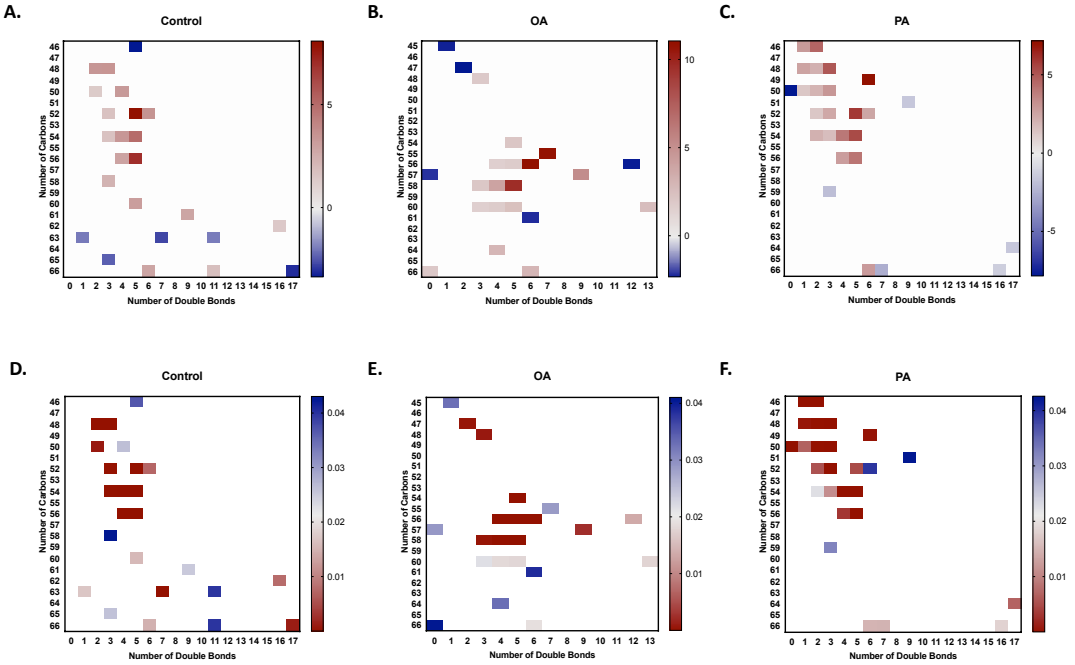

Figure 5.6 Heatmaps comparing the triglyceride profiles of PNPLA3^{KO} and PNPLA3^{UC} cells.

Heatmaps showing the (**A.-C.**) fold change difference in abundance and the (**D.-F.**) level of significance of differentially abundant triglycerides between PNPLA3^{UC} and PNPLA3^{KO} cells following the three treatments. Regardless of treatment type, the PNPLA3^{KO} cells accumulated more triglycerides containing PUFAs. In the palmitic acid treatment group, the heatmaps indicate that PNPLA3^{KO} cells may be preferentially incorporating SFAs into triglycerides as a plurality of the triglycerides that are differentially abundant between the two groups possess less than 3 double bonds.

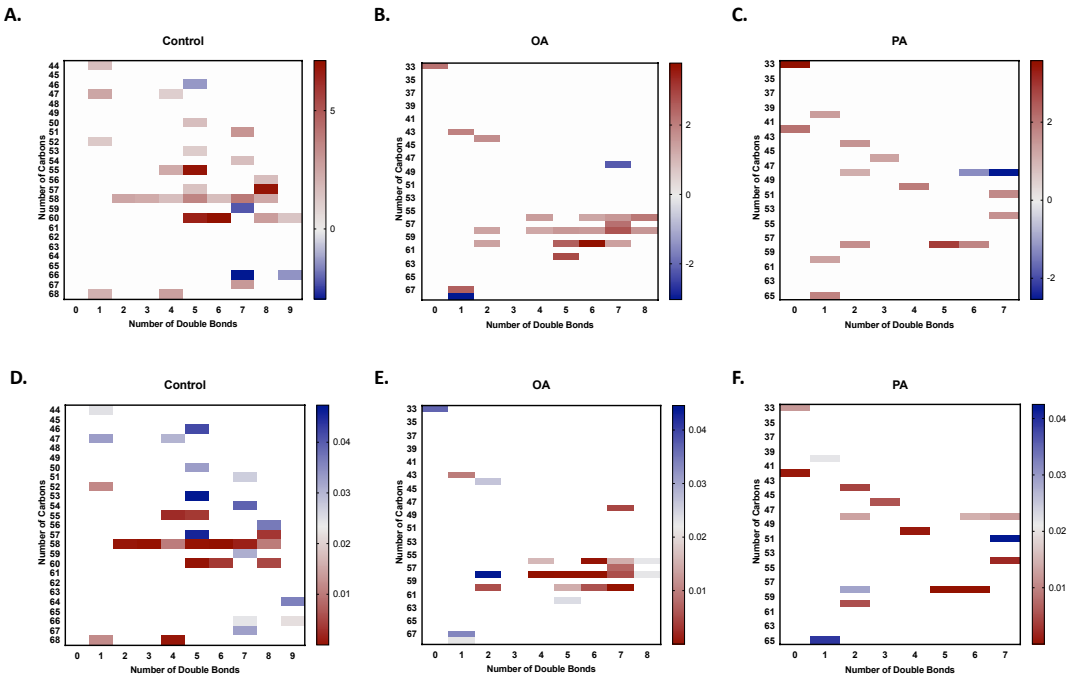

Figure 5.7 Heatmaps comparing the triglyceride profiles of PNPLA3^{I148M} and PNPLA3^{UC} cells.

Heatmaps showing the (**A.-C.)** fold change difference in abundance and the (**D.-F.**) level of significance of differentially abundant triglycerides between PNPLA3^{UC} and PNPLA3^{I148M} cells following the three treatments. Similar to the trends seen in PNPLA3^{KO} cells, the PNPLA3^{I148M} cells preferentially accumulated triglycerides containing PUFAs and when treated with palmitic acid, the PNPLA3^{I148M} cells had a higher abundance of triglycerides comprised of SFAs.

5.2.1 PNPLA3 edited lines preferentially accumulate triglycerides that contain polyunsaturated fatty acid chains

The hepatic triglycerides of carriers of the PNPLA3 I148M variant are enriched for PUFAs. PUFAs have numerous beneficial effects on lipid metabolism and have even been used as a treatment for NAFLD [252, 253]. High concentrations of PUFAs inhibit the transcription and activation of SREBP1c. PUFAs simultaneously inhibit the activation of LXRα which prevents the transcriptional upregulation of *SREBP1c* in response to insulin and increase the expression of INSIG1 protein which prevents nuclear translocation of SREBP1c [254, 255]. This reduced expression and functionality of SREBP1c leads to a downregulation of de novo lipogenesis and reduction of steatosis. Additionally, n-3 long-chain PUFAs are necessary for lipid removal from hepatocytes [81]. In addition to their role in reducing steatosis, PUFAs prevent the ER stress, apoptosis, and inflammation caused by SFAs. PUFAs accomplish this by suppressing the production of IL8 which in turn inhibits JNK and NFκB activation. This reduced JNK activity decreases ER stress markers, prevents lipoapoptosis, and reduces the release of proinflammatory mediators [81, 245-247]. Therefore, the increased relative abundance of these lipid species in the triglycerides of PNPLA3^{I148M} and PNPLA3^{KO} cells could offer insight into the resistance of these cells to palmitic acid-induced lipotoxicity.

In accordance with the clinical data, PNPLA3^{I148M} cells were enriched with triglycerides containing four to nine double bonds indicating that at least one PUFA was incorporated into the triglyceride [124, 165, 237]. A similar trend was observed in PNPLA3^{KO} cells. The PUFA species generally contain triglycerides with between 50 and 60 carbons. This is consistent with the hypothesized lipid droplet remodelling action of PNPLA3 which has a preference for catalysing the transfer of long and very long chain fatty acids from triglycerides to phospholipids [127]. The enrichment for PUFA species in triglycerides

remained consistent regardless of treatment type indicating that the role for PNPLA3 lipid droplet remodelling is independent of lipid stimuli.

The lipidomics data is also consistent with the hypothesis that the I148M variant is loss of function because the lipidomic profiles of the PNPLA3^{I148M} and PNPLA3^{KO} cells were quite similar. However, unlike the other phenotypic analyses of these cells, the PNPLA3^{I148M} cells had a more pronounced phenotype than the PNPLA3^{KO} cells. It is unclear why this would be the case. It is possible that this is a result of inter-experimental variability given that the PNPLA3^{I148M} and PNPLA3^{KO} cells were run in different mass spectrometry batches with their respective PNPLA3^{UC} controls. Alternately, this could offer evidence for the PNPLA3 I148M variant being a dominant negative variant. In this case, we use dominant negative to mean that the presence of mutated protein further exacerbates the negative effects of the loss of function variant. Previous studies have shown that I148M Pnpla3 accumulates on lipid droplets due to decreased ubiquitination [162, 163]. The presence of the I148M PNPLA3 protein may further exacerbate the negative effect of PNPLA3 loss of function on lipid droplet remodelling by further restricting the mobility of lipids or access of lipid droplet proteins. However, we did not observe the same upregulation of I148M PNPLA3 protein in our system which argues against this hypothesis. While the possibility that the I148M variant acts as a dominant negative variant remains feasible, the preponderance of evidence in our system continues to argue that the I148M variant exerts its pathogenic effects via a simple loss of enzymatic function.

	KI-Control	KI-OA	KI-PA	PNPLA3- Hyysalo Circulating	PNPLA3- Luukkonen Liver Biopsy
52:4				X	
52:6					X
54:4				X	
54:5				X	X
54:6				X	X
54:7	X		X		X
55:5	X				X
56:4		X			X
56:5				X	X
56:6		X		X	
56:7		X			X
56:8	X	X			X
58:4	X	X			X
58:5	X	X	X		X
58:6	X	X	X		X
58:7	X	X			X
58:8	X	X		X	X
58:9				X	X
60:8	X				X
60:9					X

Figure 5.8 Lipidomic comparison of PNPLA3^{I148M} cells to human patients.

Table showing upregulated triglyceride species of PNPLA3 I148M carriers in circulating samples (Hyysalo et al) and liver biopsies (Luukkonen et al) compared to PNPLA3^{I148M} lipidomic samples. The PNPLA3^{I148M} species shown in this table are triglyceride species that were differentially upregulated in PNPLA3^{I148M} cells compared to their PNPLA3^{UC} counterparts. The PNPLA3^{I148M} lipidomic profile more closely resembles the profile of liver biopsies from PNPLA3 I148M patients than the circulating lipidomic profile. The significant overlap (12/17 species) between our system and patient samples indicates the biological relevance of this system for modelling PNPLA3-induced NAFLD.

In order to validate the results from our *in vitro* system, we compared the lipidomic profile of the PNPLA3^{I148M} cells with lipidomic profiles from patients homozygous for the I148M risk allele. We used published data from Hyysalo, et al. and Luukkonen, et al. to compare the profile of our cells to patients' lipidomic profiles obtained from circulation and liver biopsy, respectively [165, 237]. Given that triglycerides were the lipid species with the largest effect on the lipidomic profile of our cells, we confined our analysis to triglycerides. The two publications found 20 triglyceride species that were upregulated in carriers of the I148M risk allele. A table of these species and their differential expression

pattern in the circulating and liver biopsy lipidome samples as well as our PNPLA3^{I148M} cells can be found in Figure 5.7. We found that of the 20 triglyceride species that were upregulated in I148M carriers, 12 were similarly upregulated in PNPLA3^{I148M} cells. As expected, the PNPLA3^{I148M} lipidome more closely resembled the sample from the liver biopsy than circulation. Of the 12 triglycerides that were upregulated in the PNPLA3^{I148M} cells, 10 were exclusively found in the lipidomic samples from patient liver biopsies. This result offers impressive clinical validation of our system. Consistent with clinical data, we have shown that the PNPLA3^{I148M} cells accumulate more lipids than their PNPLA3^{UC} counterparts and the lipidomic makeup of these prolific lipid droplets closely resemble the profile seen in the livers of patients with the I148M variant. These data demonstrate that our genetically edited HLCs recapitulate key metabolic aspects of the clinical phenotype seen in human patients and may be reliable surrogates for the effects of the I148M variant on human disease.

5.2.2 PNPLA3 edited lines incorporate lipotoxic saturated fatty acids into triglycerides

The increased concentration of triglycerides containing PUFAs could be one explanation for the decreased palmitic acid-induced lipotoxicity experienced by PNPLA3^{I148M} and PNPLA3^{KO} cells. However, there are fewer PUFA-containing triglyceride species in palmitic acid treated cells than control or oleic acid treated cells of the same genotype indicating that this is likely not the only mechanism by which PNPLA3 edited cells are avoiding lipotoxicity. Triglycerides in palmitic acid treated cells of both genotypes skew toward saturation with several species containing between zero and two double bonds. This increased triglyceride saturation in palmitic acid treated cells presents another mechanism by which PNPLA3^{I148M} and PNPLA3^{KO} cells may exhibit resistance to lipotoxicity.

SFAs have long been implicated in metabolic stress of hepatocytes due to their tendency to overwhelm β-oxidation antioxidant systems as well as triggering ER stress through hyper-saturation of membrane phospholipids. Studies have shown that metabolism of SFAs causes the accumulation of toxic intermediates and these toxic intermediates are

the culprits in lipotoxicity. SFAs stimulate their own metabolism by upregulating lipid metabolic pathways such as β-oxidation through the upregulation of PPARα expression [79-81]. Alternately, MUFAs, such as oleic acid, activate PPARγ and downstream triglyceride synthesis pathways. Therefore, somewhat paradoxically, MUFAs are not toxic to the cell because they are not metabolized to toxic intermediates but rather stored in metabolically inert triglycerides [234]. Experimental conditions that promote triglyceride synthesis such as co-supplementation of MUFAs reduces the lipotoxicity of SFAs. Therefore, if palmitic acid can be diverted into triglyceride synthesis rather than other metabolic pathways, its lipotoxic effect is neutralized [35, 231, 234].

Following this line of logic, the increased incorporation of SFAs into triglycerides in the PNPLA3^{I148M} and PNPLA3^{KO} lines treated with palmitic acid offers yet another mechanistic explanation for the reduced lipotoxic effect of palmitic acid on these cells. It appears that PNPLA3 may play a role in partitioning fatty acids between lipid storage and lipid metabolism. Loss of PNPLA3 function, either through the I148M variant or a complete knock-out, may result in a malfunction of this system. This failure to partition fatty acids has the dual effect of increasing lipid accumulation and paradoxically reducing the susceptibility of cells to lipotoxicity.

5.3 Blocking triglyceride synthesis re-sensitizes PNPLA3 edited cells to palmitic acid-induced lipotoxicity

In order to test the hypothesis that PNPLA3 edited cells escape SFA-induced lipotoxicity by rerouting them from metabolic pathways to triglyceride storage, we used small molecule inhibitors to block triglyceride formation in the cells. We hypothesized that blocking triglyceride formation would have no effect on PNPLA3^{UC} cells since they are already susceptible to palmitic acid-induced lipotoxicity. However, in PNPLA3^{I148M} and PNPLA3^{KO} cells, we hypothesized that blocking triglyceride formation would re-sensitize these cells to lipotoxicity. We chose two different small molecule inhibitors that blocked triglyceride synthesis at the top and bottom of the enzyme cascade, Triacsin C and T863, respectively. Triacsin C inhibits GPAT which is the first enzyme in the cascade while T863 inhibits DGAT1, the last enzyme in the cascade. A schematic of triglyceride formation and the impact of each of the inhibitors can be found in Figure 5.8. The

PNPLA3^{UC}, PNPLA3^{I148M}, and PNPLA3^{KO} cells were differentiated into HLCs, placed in 3D culture, and treated with either palmitic acid or palmitic acid supplemented with each inhibitor for one week. Following the treatment, viability and lipid droplet accumulation were quantified. These experiments were performed on cells from both the FSPS13B background and the A1ATDR/R background for confirmation.

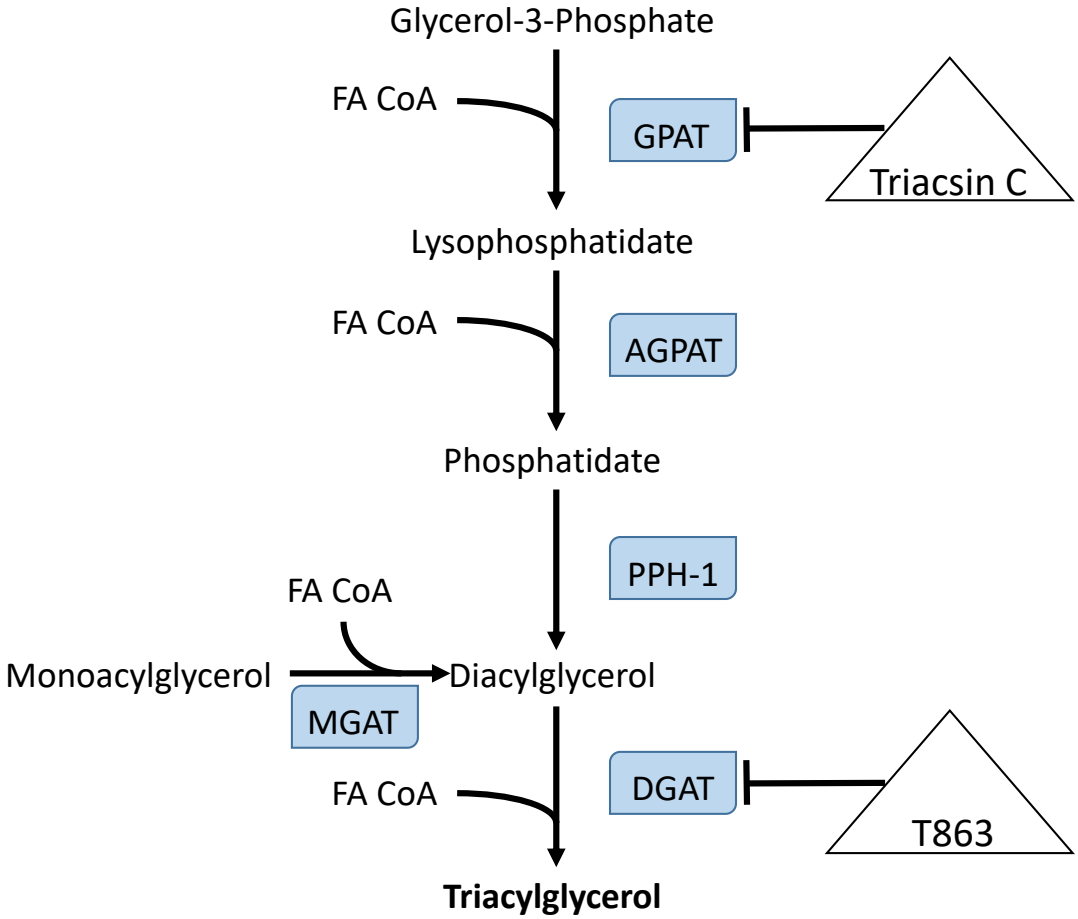

Figure 5.9 Schematic of triglyceride inhibition experiment.

Schematic of the triglyceride formation enzyme cascade denoting that Triacsin C inhibits GPAT at the top of the cascade while T863 inhibits DGAT1 at the bottom of the cascade.

Figures 5.9 and 5.10 show the results of the triglyceride blocking experiment in the FSPS13B and A1ATDR/R lines, respectively. Figure 5.9b shows that both Triacsin C and T863 reduced lipid droplet formation in all three genotypes. However, the inhibitors failed to completely inhibit triglyceride formation at the concentrations used in this

experiment. Based upon these representative images, it appears that T863 may have a stronger inhibitory effect on lipid droplet formation than Triacsin C but this qualitative observation would need to be confirmed with quantitative measurements to ensure its accuracy.

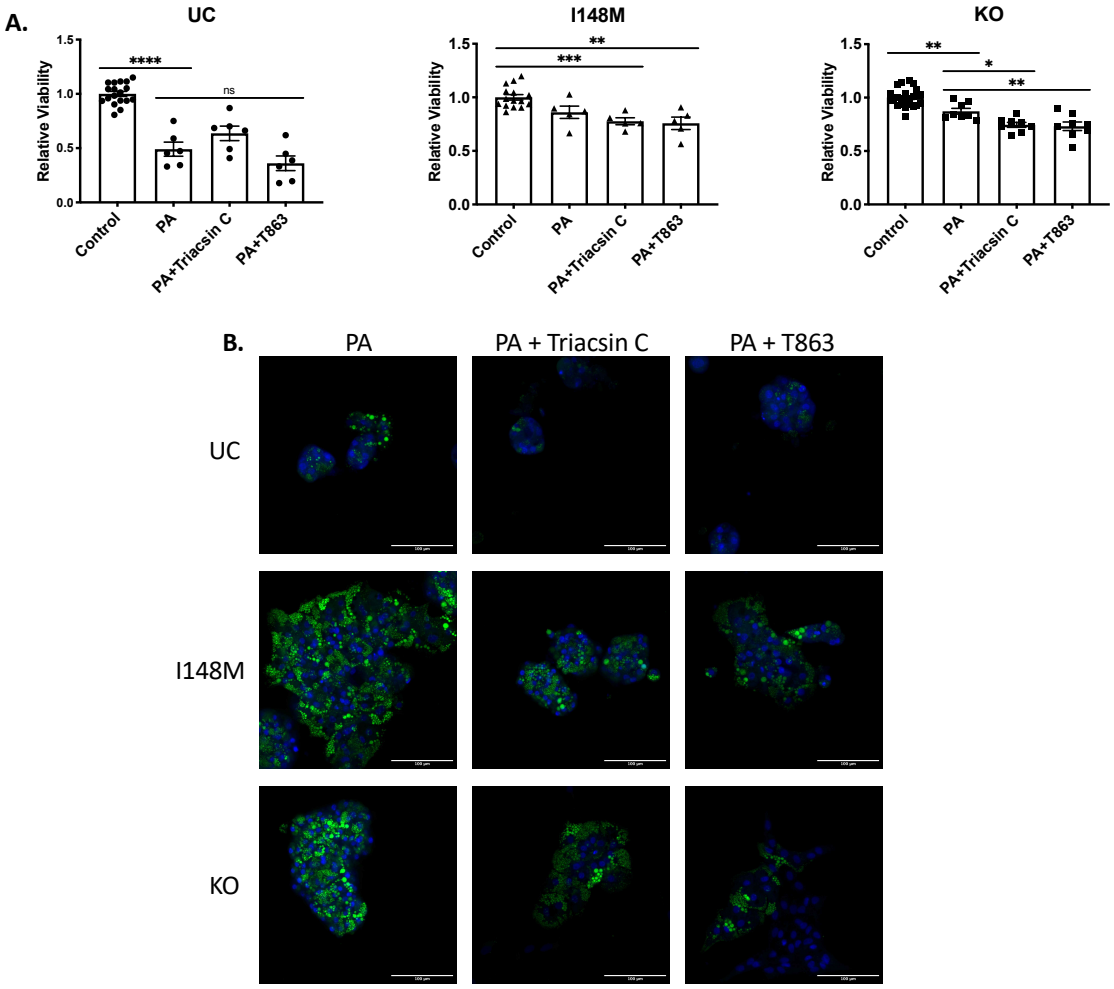

Figure 5.10 Triglyceride Blocking Assay in FSPS13B.

A. Relative viability of cells treated with palmitic acid alone or palmitic acid plus each inhibitor compared to control treated cells within each genotype ($PNPLA3^{UC}$: n = 2 clones and 3 independent experiments; $PNPLA3^{I148M}$: n = 2 clones and 3 independent experiments; $PNPLA3^{KO}$: n = 3 clones and 3 independent experiments). For $PNPLA3^{UC}$ cells, treatment with palmitic acid resulted in a significant loss of viability but treatment with the triglyceride inhibitors did not result in additional loss of viability. While treatment with both inhibitors resulted in a significant reduction in viability for $PNPLA3^{KO}$ cells. $PNPLA3^{I148M}$ cells showed an intermediate phenotype with a slight reduction in viability when treated with the triglyceride inhibitors that did not reach significance. Ordinary one-way ANOVAs with Dunnett's multiple comparisons tests were performed to test statistical significance between means. Error bars represent SEM. **B.** Representative images of bodipy lipid staining following 1 week of treatment with palmitic acid and palmitic acid supplemented with the respective inhibitors. Lipid accumulation was inhibited by both

inhibitors in all three genotypes. This experiment was performed 3 times and the best representative images are represented in this figure.

Similar to previous experiments, we found that treating PNPLA3^{UC} cells with palmitic acid resulted in a significant reduction in viability while treatment with the inhibitors did not lead to increased cell death. The PNPLA3^{KO} cells had a small but significant decrease in viability when treated with palmitic acid. Treatment with both triglyceride inhibitors resulted in significantly higher cell death than palmitic acid treatment alone. Similarly, the addition of both Triacsin C and T863 caused a significant decrease in viability in PNPLA3^{I148M} cells compared to control.

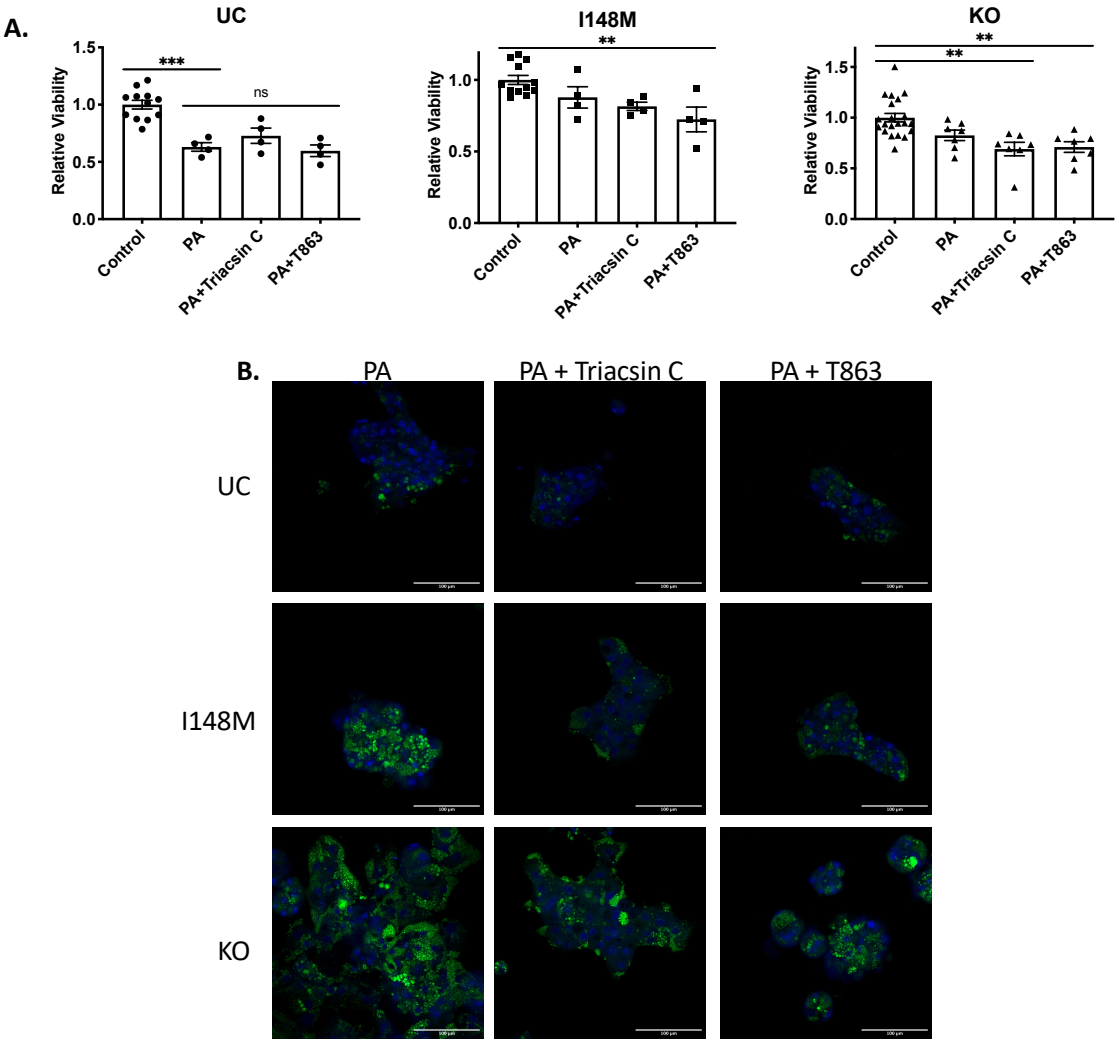

Figure 5.11 Triglyceride Blocking Assay in A1ATDR/R.

A. Relative viability of palmitic acid and palmitic acid + inhibitor treated cells to control treated cells within each genotype (PNPLA3^{UC}: n = 2 clones and 3 independent experiments; PNPLA3^{I148M}: n = 1 clone and 4

independent experiments; PNPLA3^{KO}: n = 2 clones and 4 independent experiments). The triglyceride inhibitors have less of an effect on this genetic background, but the trends remain consistent. In PNPLA3^{UC} cells, triglyceride inhibitors have no effect on further reducing the viability of palmitic acid treated cells. In PNPLA3^{I148M} and PNPLA3^{KO} cells, addition of the triglyceride inhibitors results in a slight decrease in viability when compared to palmitic acid treated cells alone. Ordinary one-way ANOVAs with Dunnett's multiple comparisons tests were performed to test statistical significance between means. Error bars represent SEM. **B.** Representative images of bodipy lipid staining following 1 week of treatment with palmitic acid and palmitic acid supplemented with the respective inhibitors. Treatment with these inhibitors resulted in a slight decrease in lipid accumulation in all three genotypes but to a lesser extent than the other genetic background. This experiment was performed 2 times and the best representative images are represented in this figure.

These results were confirmed in the A1ATDR/R genetic background. Figure 5.10b shows that the A1ATDR/R lines were more resistant to triglyceride inhibition as the cells treated with each inhibitor still had a significant amount of lipid accumulation. Accordingly, the effects on viability were less pronounced that in the FSPS13B line. The PNPLA3^{UC} line in this genetic background behaved nearly identically to FSPS13B. The viability of these cells was significantly reduced by palmitic acid treatment and treatment with the triglyceride inhibitors had no further effect on the viability of these cells. In the PNPLA3^{I148M} line, only treatment with T863 caused a significant reduction in viability. While treatment with both inhibitors caused increased cell death in the PNPLA3^{KO} cells compared to control. These results indicate that inhibiting triglyceride synthesis in PNPLA3 edited cells does re-sensitize them to palmitic acid-induced lipotoxicity.

These results support the hypothesis that mis-partitioning SFAs into storage rather than other metabolic pathways protects these cells from lipoapoptosis. However, the differences in viability between groups, though statistically significant, were small. Therefore, it is unlikely that shunting SFAs into triglycerides is the only protective mechanism at work in these cells. It remains possible that the increased concentration of PUFAs in the triglycerides of these cells and/or another unknown mechanism plays a role in PNPLA3^{I148M} and PNPLA3^{KO} cell's escape from palmitic acid induced lipotoxicity. Additional studies will be needed to fully understand the mechanisms at play that allow PNPLA3 edited cells to resist PA-induced lipotoxicity.

5.4 Conclusions

In this chapter, we used lipidomic analyses to understand the differences in lipid metabolism between $PNPLA3^{UC}$ cells and $PNPLA3^{KO}$ and $PNPLA3^{I148M}$ cells respectively. We used the lipidome of these cells to gain mechanistic insight into how $PNPLA3^{I148M}$ and $PNPLA3^{KO}$ cells accumulate more lipid droplets and escape palmitic-acid induced lipotoxicity. We found that $PNPLA3^{I148M}$ and $PNPLA3^{KO}$ cells both had starkly different lipidomic profiles than $PNPLA3^{UC}$ cells and that the PNPLA3-edited cells had similar lipidomic profiles to one another. Both $PNPLA3^{I148M}$ and $PNPLA3^{KO}$ cells preferentially sequestered triglycerides that contained PUFAs. These data were consistent with the hypothesis that PNPLA3 is a lipid droplet remodelling protein that catalyses the transfer of PUFAs between triglycerides and phospholipids. Given that both the $PNPLA3^{I148M}$ and $PNPLA3^{KO}$ cells both had increased accumulation of PUFA-containing triglycerides, these data remain consistent with the assumption that the I148M is a loss of function variant.

In addition, we compared the lipidomic profile of $PNPLA3^{I148M}$ cells to the circulating and hepatic lipidomic profiles of patients with the I148M variant to validate our system. There was a significant overlap between our system and the clinical samples. The lipidomic profile of the $PNPLA3^{I148M}$ closely resembles that of patient liver biopsy samples indicating that our cells have a competent lipid metabolism that recapitulates the phenotype observed in patients homozygous for the risk allele. These data indicate that our system has clinical relevance and may be used to gain mechanistic insight into the pathogenesis of the I148M variant.

We then used the lipidomic profiles of our cells to gain mechanistic insight into why PNPLA3-edited cells are resistant to palmitic-acid induced lipotoxicity. The lipidome of $PNPLA3^{I148M}$ and $PNPLA3^{KO}$ cells indicate that there is a dual protective effect of PUFA accumulation in triglycerides as well as preferential incorporation of SFAs into triglycerides. The presence of PUFAs in the triglycerides of these cells may prevent JNK activation and downregulate ER stress markers and inflammation while incorporation of SFAs into triglycerides may prevent the accumulation of toxic intermediates that facilitate lipotoxicity. We tested the latter hypothesis by blocking triglyceride formation in the cells

in an attempt to re-sensitized PNPLA3-edited cells to palmitic acid-induced lipotoxicity. We found that blocking triglyceride formation in PNPLA3^{I148M} and PNPLA3^{KO} cells led to a significant decrease in viability indicating that these cells are escaping palmitic acid-induced lipotoxicity, at least in part, by shuttling SFAs into metabolically inert triglycerides rather than other metabolic processes. Though the decrease in viability was statistically significant, the effect was extremely small. This small effect size may be due to an incomplete blockage of triglyceride formation at the concentrations used. Alternately, it is likely that triglyceride formation is just one mechanism by which the PNPLA3-edited cells escape palmitic acid induced lipotoxicity. Additional studies are needed to fully establish the molecular mechanism of this phenomenon. Overall, the lipidomic profile of PNPLA3-edited cells indicate that our *in vitro* system recapitulates key aspects of the human disease, offers further evidence to support the hypothesis that the I148M variant is loss of function, and sheds insight into the mechanism that prevents lipotoxicity in PNPLA3-edited cells.